ISSN 0021-8944, Journal of Applied Mechanics and Technical Physics, 2020, Vol. 61, No. 2, pp. 267–276. © Pleiades Publishing, Ltd., 2020.
Original Russian Text © N.A. Abrosimov, L.A. Igumnov, N.A. Novosel'tseva.

NUMERICAL ANALYSIS OF THE EFFECT OF STRAIN RATE ON THE DYNAMIC STRENGTH OF CYLINDRICAL METAL–PLASTIC SHELLS UNDER EXPLOSIVE LOADING

N. A. Abrosimov*, L. A. Igumnov, and N. A. Novosel'tseva

UDC 539.3

Abstract: Based on the nonclassical theory of shells, an energy-consistent resolving system of dynamics equations for metal–plastic cylindrical shells is obtained by minimizing the total-energy functional of a shell as a three-dimensional body. The numerical method for solving the formulated initial-boundary-value problem is based on an explicit variational-difference scheme. The validity of the method is confirmed by the results of comparison of numerical solutions and experimental data. The ultimate deformability and strength of homogeneous fiberglass cylindrical shells and double-layer metal–plastic shells are analyzed for various reinforcement structures.

Keywords: composite materials, cylindrical shells, strength, fracture, numerical methods, explosive loading.

DOI: 10.1134/S0021894420020133

INTRODUCTION

The use of composite materials in the manufacture of structural members subjected to intense dynamic loads has motivated experimental and theoretical studies of the effect of the strain rate of composite materials on their strength and stiffness characteristics since pulsed loading of structural members produces a stress-strain state in the material with high variability over time. The dependence of the elastic and strength characteristics of composite materials on strain rate has been noted in a number of experimental and theoretical studies [1–4]. However, determining the parameters characterizing the properties of composite materials at high strain rates is very difficult due to the need to measure the dynamic pressure on the sample as a function of time.

Theoretical study of the fracture of plates of composite materials taking into account the effect of strain rate on the deformation and strength characteristics of these materials was carried out in [5]. It should be noted that the results of studying this dependence and features of nonlinear dynamic deformation and fracture of composite materials can be used in the development of methods for reducing the material content of structural members operating under intense dynamic loading. This has motivated the further development of theoretical and experimental methods [6–8] for studying unsteady processes in composite materials and structural members at their ultimate load-bearing capacity.

In this paper, we study the effect of strain rate on the dynamic loading behavior and fracture of cylindrical shells made of metal–plastic materials.

Research Institute of Mechanics, Lobachevsky National Research Nizhny Novgorod State University, Nizhny Novgorod, 603950 Russia; *abrosimov@mech.unn.ru; igumnov@mech.unn.ru; novoselceva@mech.unn.ru. Translated from Prikladnaya Mekhanika i Tekhnicheskaya Fizika, Vol. 61, No. 2, pp. 130–141, March–April, 2020. Original article submitted July 18, 2019; revision submitted August 16, 2019; accepted for publication September 30, 2019.
*Corresponding author.

1. FORMULATION OF THE PROBLEM AND METHODS FOR ITS SOLUTION

Cylindrical shells of length L and radius R are investigated in the coordinate system α_i ($i = \overline{1,3}$) where the axis α_1 is directed along the generatrix, the axis α_2 along the circle, and the axis α_3 along the external normal to the median surface. The Lamé coefficients and the principal curvatures are $H_1 = Z_1 = 1$, $H_2 = Z_2 = 1 + k_2\alpha_3$, $H_3 = 1$, $k_1 = 0$, and $k_2 = 1/R$. We considered homogeneous fiberglass shells obtained by winding alternating double spiral and annular layers with a thickness ratio of 1 : 1 and inhomogeneous shells obtained by spiral cross winding of unidirectional fiberglass (according to the reinforcement scheme of homogeneous shells) on a steel cylindrical mandrel of low carbon steel.

The kinematic model for the deformation of an inhomogeneous multilayer package is based on the nonclassical theory of shells. The components of the displacement vector are approximated by finite series along the thickness of the multilayer package [9]:

$$u_i(\alpha_1, \alpha_3, t) = \sum_{n=0}^{N} u_i^n(\alpha_1, t)\Big(n + \frac{1}{2}\Big)^{1/2} P_n(x), \qquad x = \frac{2\alpha_3}{h}, \quad -1 \leqslant x \leqslant 1 \tag{1}$$

[h is the shell thickness, $u_i^n(\alpha_1, t)$ are the desired functions, t is time, and $(n + 1/2)^{1/2}P_n(x)$ are the orthonormal Legendre polynomials].

Geometric dependences are formulated using the relations of the quadratic nonlinear theory of elasticity in curvilinear coordinates [10], which, in view of (1), can be represented as

$$e_{11} = \sum_{n=0}^{N} \frac{\partial u_1^n}{\partial \alpha_1}\Big(n + \frac{1}{2}\Big)^{1/2} P_n(x) + \frac{1}{2}\,\omega_2^2, \qquad e_{22} = \frac{k_2}{Z_2}\sum_{n=0}^{N} u_3^n\Big(n + \frac{1}{2}\Big)^{1/2} P_n(x),$$

$$e_{33} = \frac{2}{h}\sum_{n=1}^{N} u_3^n\Big(n + \frac{1}{2}\Big)^{1/2} P_n'(x), \quad e_{13} = \frac{2}{h}\sum_{n=1}^{N} u_1^n\Big(n + \frac{1}{2}\Big)^{1/2} P_n'(x) + \sum_{n=0}^{N} \frac{\partial u_3^n}{\partial \alpha_1}\Big(n + \frac{1}{2}\Big)^{1/2} P_n(x),$$

$$\omega_2 = \frac{1}{2}\Big(\frac{2}{h}\sum_{n=1}^{N} u_1^n\Big(n + \frac{1}{2}\Big)^{1/2} P_n'(x) - \sum_{n=0}^{N} \frac{\partial u_3^n}{\partial \alpha_1}\Big(n + \frac{1}{2}\Big)^{1/2} P_n(x)\Big),$$

where $P_n'(x)$ are the derivatives of the Legendre polynomials.

The relationship between the stress and strain tensors in a homogeneous composite macrolayer is established on the basis of Hooke's law for an orthotropic body using the theory of effective moduli [11]:

$$\sigma_{ii} = \sum_{j=1}^{3} C_{ij} e_{jj} \quad (i = \overline{1,3}), \qquad \sigma_{13} = G_{13} e_{13}.$$

Here C_{ij}, G_{13} are the effective stiffness characteristics of symmetric adjacent layers, which are expressed in terms of the elastic moduli E_{ij} and Poisson's ratios ν_{ij} of the unidirectional composite material.

The layer-by-layer fracture of layered cylindrical shells is described using the model of degradation of their stiffness characteristics [12]. In addition, the dependence of the strength characteristics of composite materials on strain rate is taken into account. In particular, for unidirectional fiberglass [5], the stiffness and strength characteristics of the material can be described by the regression function

$$F(\dot{e}) = \alpha + \beta \dot{e}^{\gamma}, \tag{2}$$

where F and $\dot{e}$ are the strength characteristics and the strain rate, respectively, and α, β, and γ are experimentally determined material constants.

The constitutive relations in the isotropic steel layer of the shell are formulated on the basis of the differential theory of plasticity with linear hardening [9]:

$$\sigma_{ij} = \frac{\nu E}{(1+\nu)(1-2\nu)}\, e + \frac{E}{2(1+\nu)}\, e'_{ij},$$

$$e_{ij} = e'_{ij} + e''_{ij}, \quad e = e_{11} + e_{22} + e_{33}, \quad \dot{e}_{ij} = \dot{\gamma} S_{ij}, \quad \sigma = (\sigma_{11} + \sigma_{22} + \sigma_{33})/3,$$

$$\sum_{i,j=1}^{3} S_{ij}S_{ij} = \frac{2}{3}\,\sigma_*^2, \quad S_{ij} = \sigma_{ij} - \sigma\delta_{ij} - \rho_{ij}, \quad \rho_{ij} = 2ge''_{ij}, \quad e''_{ij} = \int\limits_0^t \dot{e}''_{ij}\,dt$$

(E is the elastic modulus, ν is the Poisson's ratio, e'_{ij} and e''_{ij} are the elastic and plastic components of the strain tensor, δ_{ij} is the Kronecker tensor, σ_*, g is the yield point and the hardening modulus of the material, and $\dot{\gamma}$ is a scalar parameter).

The energy-consistent system of motion equations for a a metal–plastic shell is constructed based on the principle of possible displacements [13]. For a cylindrical shell with free edges loaded by an internal pressure pulse, it is written as

$$\int\limits_0^L \sum_{n=0}^{N} \Big(M_{11}^n\,\frac{\partial\,(\delta u_1^n)}{\partial\alpha_1} + (M_{13}^{\prime n} + N_{11}^{\prime n})\,\delta u_1^n + (M_{13}^n - N_{11}^n)\,\frac{\partial\,(\delta u_3^n)}{\partial\alpha_1} + (k_2M_{22}^n + M_{33}^n)\,\delta u_3^n\Big)\,d\alpha_1$$

$$+ \int\limits_0^L \sum_{n=0}^{N} \Big[\Big(\sum_{m=0}^{N} A_m^n\ddot{u}_1^m\Big)\,\delta u_1^n + \Big(\sum_{m=0}^{N} A_m^n\ddot{u}_3^m\Big)\delta u_3^n\Big]\,d\alpha_1 - \int\limits_0^L \sum_{n=0}^{N} F_3^n\,\delta u_3^n\,d\alpha_1 = 0, \tag{3}$$

where

$$M_{11}^n = \frac{h}{2}\sum_{i=1}^{K}\frac{x_{i+1}-x_i}{2}\int\limits_{-1}^{1}\sigma_{11}Z_2\Big(n+\frac{1}{2}\Big)^{1/2}P_n\Big(\frac{x_{i+1}-x_i}{2}\,x + \frac{x_{i+1}+x_i}{2}\Big)\,dx,$$

$$M_{22}^n = \frac{h}{2}\sum_{i=1}^{K}\frac{x_{i+1}-x_i}{2}\int\limits_{-1}^{1}\sigma_{22}\Big(n+\frac{1}{2}\Big)^{1/2}P_n\Big(\frac{x_{i+1}-x_i}{2}\,x + \frac{x_{i+1}+x_i}{2}\Big)\,dx,$$

$$M_{13}^n = \frac{h}{2}\sum_{i=1}^{K}\frac{x_{i+1}-x_i}{2}\int\limits_{-1}^{1}\sigma_{13}Z_2\Big(n+\frac{1}{2}\Big)^{1/2}P_n\Big(\frac{x_{i+1}-x_i}{2}\,x + \frac{x_{i+1}+x_i}{2}\Big)\,dx,$$

$$M_{13}^{\prime n} = \frac{h}{2}\sum_{i=1}^{K}\frac{x_{i+1}-x_i}{2}\int\limits_{-1}^{1}\sigma_{13}Z_2\Big(n+\frac{1}{2}\Big)^{1/2}P'_n\Big(\frac{x_{i+1}-x_i}{2}\,x + \frac{x_{i+1}+x_i}{2}\Big)\,dx,$$

$$N_{11}^n = \frac{h}{4}\sum_{i=1}^{K}\frac{x_{i+1}-x_i}{2}\int\limits_{-1}^{1}\sigma_{11}Z_2\omega_2\Big(n+\frac{1}{2}\Big)^{1/2}P_n\Big(\frac{x_{i+1}-x_i}{2}\,x + \frac{x_{i+1}+x_i}{2}\Big)\,dx,$$

$$N_{11}^{\prime n} = \frac{1}{2}\sum_{i=1}^{K}\frac{x_{i+1}-x_i}{2}\int\limits_{-1}^{1}\sigma_{11}Z_2\omega_2\Big(n+\frac{1}{2}\Big)^{1/2}P''_n\Big(\frac{x_{i+1}-x_i}{2}\,x + \frac{x_{i+1}+x_i}{2}\Big)\,dx,$$

$$M_{33}^n = \frac{h}{4}\sum_{i=1}^{K}\frac{x_{i+1}-x_i}{2}\int\limits_{-1}^{1}\sigma_{33}Z_2\omega_2\Big(n+\frac{1}{2}\Big)^{1/2}P'_n\Big(\frac{x_{i+1}-x_i}{2}\,x + \frac{x_{i+1}+x_i}{2}\Big)\,dx,$$

$$A_n^n = \frac{1}{2}\sum_{i=1}^{K}\rho_i(x_{i+1}-x_i) \quad (n = \overline{0,N}\,),$$

$$A_{n+1}^n = A_n^{n+1} = \frac{k_2(n+1)}{4\sqrt{4n^2+8n+3}}\sum_{i=1}^{K}\rho_i(x_{i+1}-x_i)^2 \quad (n = \overline{0,N-1}\,),$$

$$A_m^n = 0 \quad \text{for} \quad n \neq m \quad (m = \overline{0,N},\ n = \overline{0,N}),$$

$$F_3^n = (n+1/2)^{1/2}(-1)^n p_3(1-k_2h/2),$$

ρ_i is the density of the ith layer of the shell, p_3 is the intensity of the internal pressure pulse, K is the number of shell layers, and x_i is the coordinate of the ith layer measured from the inner surface of the shell along the thickness.

Using the standard procedure for minimizing the total energy functional (3), we obtain non-classical equations of motion for the metal–plastic cylindrical shell

$$\begin{gathered}\frac{\partial M_{11}^n}{\partial \alpha_1} - M_{13}^{\prime n} - N_{11}^{\prime n} = \sum_{m=0}^{N} A_m^n \ddot{u}_1^m, \\ \frac{\partial \left(M_{13}^n - N_{11}^n\right)}{\partial \alpha_1} - k_2 M_{22}^n - M_{33}^n + F_3^n = \sum_{m=0}^{N} A_m^n \ddot{u}_3^m\end{gathered} \tag{4}$$

and natural boundary conditions for $\alpha_1 = 0, L$:

$$M_{11}^n = 0, \qquad M_{13}^n - N_{11}^n = 0. \tag{5}$$

The basic equations (4) and (5) are integrated subject to the initial conditions written as

$$u_i^n(\alpha_1, 0) = u_i^{0n}(\alpha_1), \qquad \dot{u}_i^n(\alpha_1, 0) = \dot{u}_i^{0n}(\alpha_1) \qquad (i = 1, 3, \quad n = \overline{0,N}),$$

where $u_i^{0n}(\alpha_1)$ and $\dot{u}_i^{0n}(\alpha_1)$ are the moments of the specified functions $u_i^0(\alpha_1, \alpha_3)$ and $\dot{u}_i^0(\alpha_1, \alpha_3)$ defined by the formulas

$$u_i^{0n}(\alpha_1) = \int_{-1}^{1} u_i^0(\alpha_1, \alpha_3)\Big(n+\frac{1}{2}\Big)^{1/2} P_n(x)\,dx, \qquad \dot{u}_i^{0n}(\alpha_1) = \int_{-1}^{1} \dot{u}_i^0(\alpha_1, \alpha_3)\Big(n+\frac{1}{2}\Big)^{1/2} P_n(x)\,dx.$$

The obtained equations are universal because they can be used to describe nonlinear unsteady deformation processes and evaluate the ultimate deformability and strength of two-layer metal–plastic cylindrical shells, whose geometric and structural parameters vary over wide ranges.

The numerical method for solving the formulated problem is based on an explicit variational-difference scheme [14]. The calculations were carried out on the Lobachevsky supercomputer.

2. RESEARCH RESULTS

In the numerical analysis of the effect of strain rate on the dynamic strength of two-layer metal–plastic cylindrical shells, we investigated the their deformation under the action of a pressure pulse caused by an explosion in the center of the shell of an explosive charge. The pressure profile in the incident shock wave is described by the empirical dependence [15]

$$p_3(\alpha_1, t) = \begin{cases} 0.35mq/l^3, & t \leqslant 0.35l/\sqrt{q}, \\ 0, & t > 0.35l/\sqrt{q} \end{cases}$$

(m is the mass of the charge, $q = 4.77 \cdot 10^6$ J/kg is the heat capacity of the explosive, l is the distance from the center of the charge to a point on the inner surface of the shell).

We considered both homogeneous fiberglass shells and double-layer metal–plastic cylindrical shells of length $L = 4R$ and thickness $h = h_1 + h_2$ (inner steel layer of thickness $h_1 = 0.002$ m and an outer fiberglass macro layer of thickness h_2). The physico-mechanical characteristics of fiberglass with unidirectional reinforcement were determined from the results of quasistatic tests of annular and planar unidirectional specimens using standard methods for identification of stiffness and strength characteristics [8]. For unidirectional fiberglass, the stiffness and strength characteristics in tension and compression had the following values: $E_{11} = 55$ GPa, $E_{22} = E_{33} = 9.04$ GPa, $\nu_{12} = \nu_{23} = 0.276$, $\nu_{13} = 0.4$, $G_{12} = G_{13} = 5.08$ GPa, $G_{23} = 5.2$ GPa, $\rho = 2057$ kg/m^3, $F_{11}^{\text{st}} = 1.5$ GPa, $F_{11}^{\text{str}} = 0.397$ GPa, $F_{22}^{\text{st}} = 0.0267$ GPa, $F_{22}^{\text{str}} = 0.0719$ GPa, $F_{33}^{\text{st}} = 0.0267$ GPa, $F_{33}^{\text{str}} = 0.0719$ GPa,

Table 1. Material constants in the regression function (2)

Strength characteristics, GPa	α	β	γ
F_{11}^{st}	1.50000	0.0146951	0.8860
F_{11}^{str}	0.39700	0.5154558	0.0874
$F_{22}^{\mathrm{st}} = F_{33}^{\mathrm{st}}$	0.02670	0.0080424	0.1310
$F_{22}^{\mathrm{str}} = F_{33}^{\mathrm{str}}$	0.07190	0.0000719	1.2780
$F_{12} = F_{23} = F_{13}$	0.00357	0.0178477	0.0860

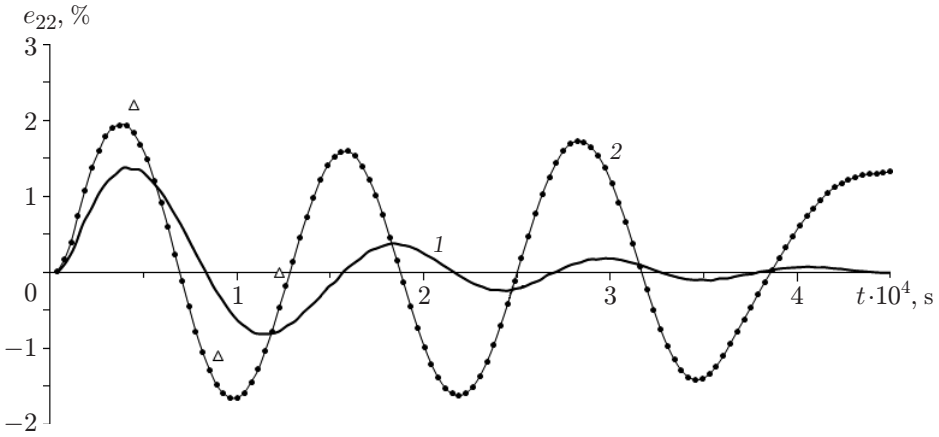

Fig. 1. Dependence of circumferential strains on time for $\alpha_1 = L/2$ and $\alpha_3 = h/2$: points refer to the experimental results and curves to the results of numerical calculations; (*1*) fiberglass-based metal–plastic shells; (*2*) homogeneous fiberglass shells.

$F_{12} = 0.0357$ GPa, $F_{23} = 0.0357$ GPa, and $F_{13} = 0.0357$ GPa. The parameters of the differential theory of plasticity of the steel layer were $E = 210$ GPa, $\nu = 0.3$, $\sigma_* = 0.35$ GPa, $g = 0.5$ GPa, and $\rho = 7800$ kg/m^3.

The dependence of the strength characteristics of unidirectional fiberglass on strain rate is described by the function (2), whose parameters are given in Table 1 (F_{ii}^{st}, F_{ii}^{str}, and F_{ij} are the initial strength characteristics in tension and compression) [5].

Oscillograms of circumferential strains in the central section on the outersurface of unfractured fiberglass and metal–plastic shells loaded by an explosive charge of mass $m = 23.8$ g are given in Fig. 1. It is seen that the presence of the plastically deforming, reinforcing steel layer leads to rapid attenuation of oscillations in the central zone of the shell and, as a result, to a significant reduction in circumferential strain, leading to an increase in the load-bearing capacity of metal–plastic shells.

Tables 2–4 show the results of numerical and experimental analysis of the ultimate deformability and fracture of fiberglass and metal–plastic shells with various reinforcement structures (e_{22}^* is the maximum circumferential strain in the central section on the outer surface of the shell, t^* is the time at which it is reached, and T is the period of radial oscillations of the lowest mode).

From an analysis of the data in Tables 2 and 3, it follows that in the case of fiberglass shells, there is a substantial increase in the ultimate strain and specific strength in the case where a steel shell is inserted into the composite shell. In this case, fracture of shells with an annular reinforcement structure of the composite macro layer occurs at lower ultimate strains compared to shells consisting of annular and spiral elementary layers.

It follows from Table 4 that accounting for the dependence of strength characteristics on strain rate leads to a change in the fracture pattern of cylindrical shells. Shells with an annular reinforcement structure have the lowest bearing capacity.

Figure 2–6 shows the fracture process at different times for metal–plastic shells loaded with an explosive charge of mass $m = 334.5$ g with different reinforcement structures in the cases where the strength characteristics are constant or depend on the strain rate.

Table 2. Calculated and experimental data [16] for homogeneous fiberglass shells (reinforcement structure $[\pm 65°; 90°]$)

R, m	h/R, %	m, g	Experiment				Calculation			
			e^*_{22}, %	t^*, μs	T, μs	State of shell	e^*_{22}, %	t^*, μs	T, μs	State of shell
0.1525	6.50	206	1.90	65	195	Intact with damage	2.30	61,5	—	Fractured in the first oscillation period in the compression phase
0.1546	6.02	208	2.15	73	195	Fractured in the third oscillation period in the compression phase	2.56	62.0	—	Fractured in the first oscillation period in the compression phase
0.1548	6.19	264	2.20	75	205	Fractured in the third oscillation period in the compression phase	3.16	64.0	—	Fractured in the first oscillation period in the compression phase
0.1549	6.38	466	3.90	70	—	Fractured in the first oscillation period in the compression phase	4.50	43.9	—	Fractured in the extension phase
0.1547	6.06	483	5.20	75	—	Fractured in the extension phase	4.82	41.6	—	Fractured in the extension phase

Table 3. Calculated and experimental data [16] for fiberglass-based metal–plastic shells (reinforcement structure $[\pm 45°; 90°]_8$) for $R = 0.1529$ m, $h/R = 7.11\%$, $m = 334.5$ g

Method of data acquisition	e^*_{22}, %	t^*, μs	State of shell
Experiment	3.90	95	Intact with damage to the steel shell
Calculation at constant strength characteristics	3.94	130	Fractured in the first oscillation period
Calculation taking into account the dependence of strength characteristics on strain rate	2.95	87	Intact with partial damage to all layers

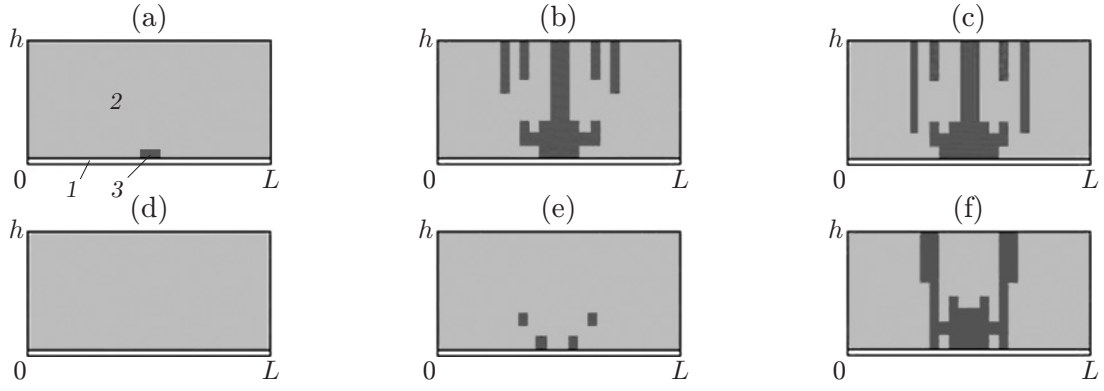

Fig. 2. Fracture of metal–plastic shells with the reinforcement structure $[\pm 30°]$ in the case of constant strength characteristics (a–c) and in the case of strength characteristics dependent on strain rate (d–f) for $t = 0.000185$ (a and d), 0.000259 (b and e), and 0.000395 s (c and f); (*1*) zones without fracture; (*2*) matrix fracture zones; (*3*) fiber fracture zones.

Table 4. Calculation results for metal–plastic shells with different reinforcement structures for $R = 0.1529$ m, $h/R = 7.11\%$, and $m = 334.5$ g

Reinforcement structure	State of shell	
	Calculation for constant strength characteristics	Calculation taking into account the dependence of strength characteristics on strain rate
[±30°]	Fractured in the first period of oscillations in the extension phase	Fractured in the first period of oscillations in the extension phase
[±45°]	Fractured in the first oscillation period in the extension phase	Intact with partial damage to all layers
[90°]	Fractured in the first oscillation period in the compression phase	Fractured in the first oscillation period in the compression phase
[±30°; 90°]	Fractured in the first oscillation period in the extension phase	Intact with partial damage to all layers
[±45°; 90°]	Fractured in the first oscillation period in the extension phase	Intact with partial damage to all layers

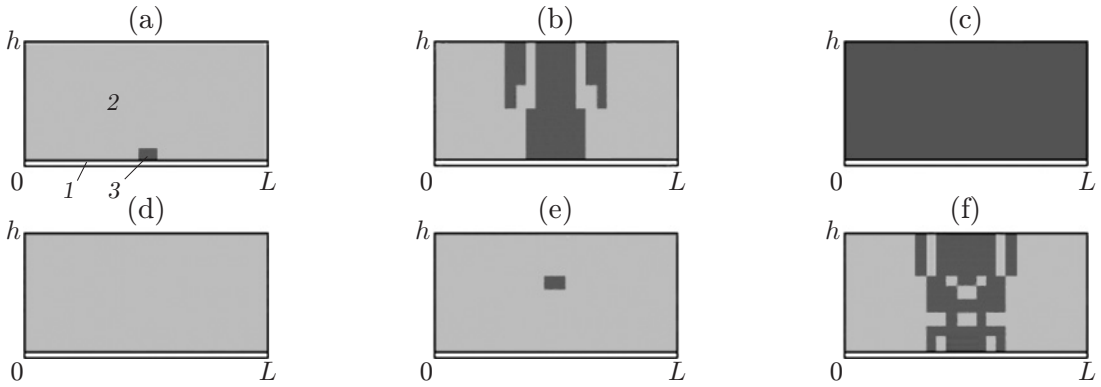

Fig. 3. Fracture of metal–plastic shells with the reinforcement structure [±45°] for $t = 0.000216\,41$ (a and d), 0.00024115 (b and e), and $t = 0.001$ s (c and f); the remaining notation the same as in Fig. 2.

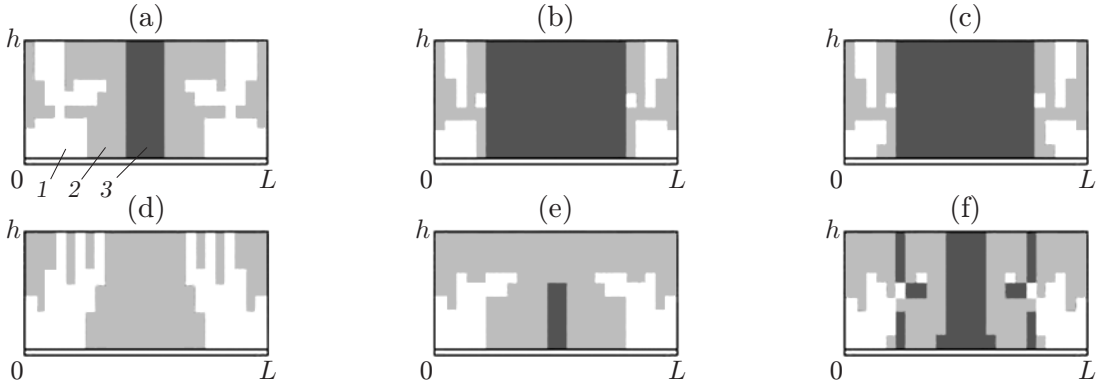

Fig. 4. Fracture of metal–plastic shells with the reinforcement structure [±90°] for $t = 0.00014830$ (a and d), 0.00018549 (b and e), and 0.00019168 s (c and f); the remaining notation the same as in Fig. 2.

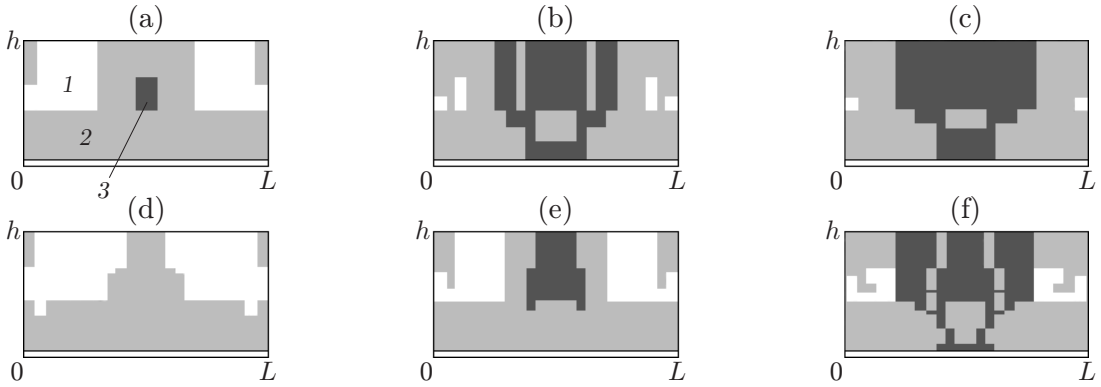

Fig. 5. Fracture of metal–plastic shells with the reinforcement structure $[\pm 30^\circ; 90^\circ]$ for $t = 0.0000618$ (a and d), 0.00021 (b and e), and 0.001 s (c and f); the remaining notation the same as in Fig. 2.

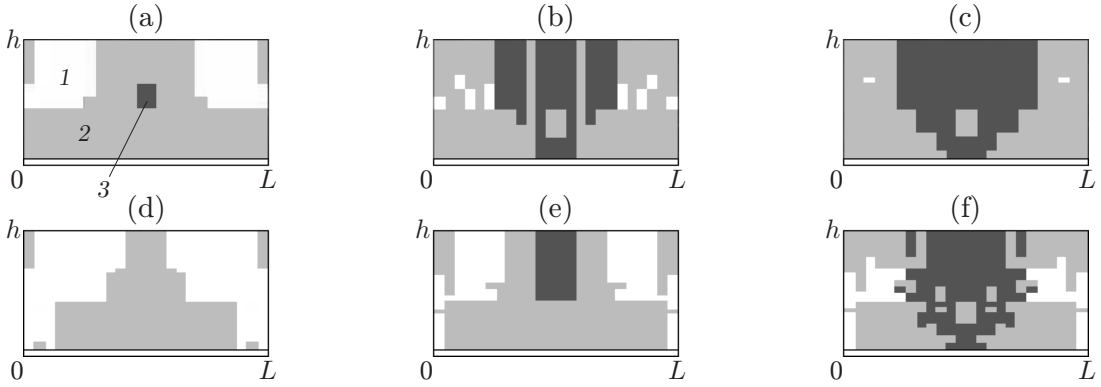

Fig. 6. Fracture of metal–plastic shells with a reinforcement structure $[\pm 45^\circ; 90^\circ]$ for $t = 0.0000618$ (a and d), 0.000204 (b and e), and 0.001 (c and f); the remaining notation the same as in Fig. 2.

Figures 2–4 show the zones of local fracture of the binder and fibers for cylindrical shells with a homogeneous cross winding structure at angles of ±30, ±45, and ±90° to the generatrix of the shell, respectively, at different times. It is seen that the angle of reinforcement and the dependence of the strength characteristics on strain rate have a significant effect on the nature and size of the fracture zones and the time at which complete fracture of the shell (fracture of fibers throughout the shell thickness) occurs.

Figures 5 and 6 show the fracture of shells with a two-layer reinforcement structure, whose outer layer is obtained by annular winding and whose inner layer is obtained by spiral cross winding at angles of ±30° and ±45°. It can be seen that the fracture of fibers begins in the outer annular layer, then fracture of the fibers of the lower layer, and complete fracture of the shells, reinforced at angles of ±30° occurs at large times compared to shells reinforced at angles of ±45°. In addition, taking into account the dependence of strength characteristics on strain rate does not lead to complete fracture of the shell.

The obtained results indicate that for all reinforcement structures calculation taking into account the dependence of strength characteristics on strain rate leads to a change in the nature and size of the fracture zones of the binder and fibers as well to a significant increase in the carrier ability of shells in comparison with calculation at constant strength characteristics.

Figure 7 shows the calculated and experimental dependences [8] of the maximum circumferential strain e_{22}^* on the specific explosive load $m_* = m/M_{\text{shell}}$ (M_{shell} is the mass of the shell for metal–plastic shells whose composite macrolayer is made of fiberglass. It is seen that the dependences $e_{22}^*(m_*)$ are linear up to the moment of fracture.

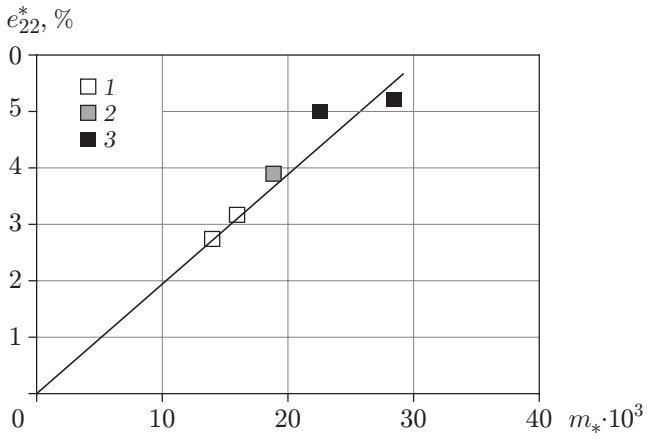

Fig. 7. Calculated (curve) and experimental (points) dependence of the maximum circumferential strain of metal–plastic shells on specific explosive load: (*1*) state where the shell is intact; (*2*) state where the shell is partially fractured; (*3*) state where the shell is completely fractured.

The increase in the difference between the theoretical and experimental results with increasing relative mass of the charge is apparently due to the imperfection of the fracture model.

The results indicate the high specific strength of pulse-loaded metal–plastic shells, which is in good agreement with experimental data [8, 16].

CONCLUSIONS

Computational models were proposed that can be used to analyze the fracture of dynamically loaded cylindrical metal–plastic shells with consideration of the strain rate dependence of their strength characteristics (dynamic model) as well as for constant characteristics (static model). The results of calculations using the dynamic and static models were compared with experimental data. It is shown that the results of calculations for the dynamic model are in better agreement with experimental data. Differences in the pattern and size of fracture regions calculated using the dynamic and static models were identified for different reinforcement structures of the composite macrolayer.

The results can be used in the design of load-bearing members of protective structures and evaluation of their dynamic strength.

The development of the deformation model was supported by the Russian Science Foundation (project code 16-19-10237-P), and the development of the fracture model by the Russian Foundation for Basic Research (Grant Nos. 18-08-01234 and 19-08-00828).

REFERENCES

1. A. G. Demeshkin, "Experimental Investigation of the Effect of Strain Rate on the Strength Characteristics of Glass–Epoxy Rings," Mekh. Kompoz. Mater., No. 3, 455–460 (1990).
2. A. V. Aseev, G. E. Makarov, and S. V. Stepanenko, "Experimental Investigation of the Dynamic Behavior of Tubular Samples of Composite Fiber Materials at the Limit of Carrying Capacity," Prikl. Mekh. Tekh. Fiz. **33** (3), 140–147 (1992) [J. Appl. Mech. Tech. Phys. **33** (3), 447–454 (1992)].
3. A. V. Aseev, N. N. Gorshkov, A. G. Demeshkin, et al., "Experimental Study of the Deformability of Glass and Organic Plastics as a Function of Strain Rate," Mekh. Kompoz. Mater., No. 2, 188–195 (1992).
4. A. A. Korobkov, A. I. Alatortsev, Yu. V. Girin, et al., "Unsteady Deformation and Fracture of Composite Shells under Thermal Force Loading," Global Nauch. Potentsial, No. 6, 37–49 (2014).

5. M. M. Shokrieh and A. Karamnejad, "A Investigation of Strain Rte Effects on the Dynamic Response of a Glass/Epoxy Composite Plate under Blast Loading by using the Finite-Difference Method," Mech. Compos. Mater. **50** (3), 295–310 (2014).
6. A. G. Fedorenko, M. A. Syrunin, and A. G. Ivanov, "Criteria for Selecting Composite Materials for Explosion Containment Structures (Review)," Fiz. Goreniya Vzryva **41** (5), 3–13 (2005) [Combust., Expl., Shock Waves **41** (5), 487–495 (2005)].
7. A. G. Ivanov, M. A. Syrunin, and A. G. Fedorenko, "Effect of Reinforcing Structures on the Critical Deformability and Strength of Shells Made of Oriented Glass-Plastic Composites under an Internal Explosive Load," Prikl. Mekh. Tekh. Fiz. **33** (4), 130–135 (1992) [J. Appl. Mech. Tech. Phys. **33** (4), 594–598 (1992)].
8. V. N. Rusak, A. G. Fedorenko, M. A. Syrunin, et al., "Limiting Deformability and Strength of Basalt Plastic Shells under Internal Explosive Loading," Prikl. Mekh. Tekh. Fiz. **43** (1), 186–195 (2002) [J. Appl. Mech. Tech. Phys. **43** (1), 154–163 (2002)].
9. N. A. Abrosimov and V. G. Bazhenov, *Nonlinear Problems of the Dynamics of Composite Structures* (Nizhny Novgorod State Univ., Nizhny Novgorod, 2002) [in Russian].
10. L. A. Shapovalov, "On the Account of Transverse Compression in the Equations of Nonlinear Dynamics of Shells," Izv. Ross. Akad. Nauk, Mekh. Tverd. Tela, No. 3, 156–168 (1997).
11. A. K. Malmeister, V. P. Tamuzh, and G. A. Teters *The Strength of Polymer and Composite Materials* (Zinatne, Riga, 1980) [in Russian].
12. N. A. Abrosimov and N. A. Novosel'tseva, "Numerical Simulation of the Layer-by-Layer Destruction of Cylindrical Shells under Explosive Loading," Mekh. Kompoz. Mater. **51** (4), 579–594 (2015) [Mech. Compos. Mater. **51** (4), 407–418 (2015)].
13. K. Washizu, *Variational Methods in Elasticity and Plasticity* (Pergamon Press, Oxford (1982)].
14. N. A. Abrosimov, A. V. Elesin, L. N. Lazarev, and N. A. Novosel'tseva, "Numerical Analysis of the Strength of Fiberglass Cylindrical Shells of Different Structure under Pulsed Loading," Probl. Prochn. Plastich., No. 75, 288–295 (2013).
15. V. V. Adishchev, V. M. Kornev, and L. A. Talzi, *Estimates of Maximum Stresses in Closed Cylindrical Vessels under Axisymmetric Explosive Loading* (Institute of Hydrodynamics, Siberian Branch, USSR Academy of Sciences, Novosibirsk, 1983). Deposited at VINITI May 12, 1983, No. 6588-83.
16. A. G. Ivanov M. A. Syrunin, and A. G. Fedorenko, "Effect of the Reinforcing Structure on the Critical Deformability and Strength of Shells Made of Oriented Glass-Plastics Composites under an Internal Explosive Load," Prikl. Mekh. Tekh. Fiz. **33** (4), 130–135 (1992) [J. Appl. Mech. Tech. Phys. **33** (4), 594–597 (1992)].